RSC Advances

ROYAL SOCIETY OF CHEMISTRY

www.rsc.org/advances

Highly moisture-resistant epoxy composites: An approach based on liquid nano-reinforcement containing well-dispersed activated montmorillonite

Xiaolong Jia[a, b], Junyi Zheng[a], Song Lin[c], Wenbin Li[a], Qing Cai[a, *], Gang Sui[a], Xiaoping Yang[a, b]

Abstract:

Effects of butyl glycidyl ether (BGE) activated montmorillonites (BGE-MMTs) on moisture-resistant characteristics of epoxy-based composites were evaluated. The activated MMTs were prepared by intercalating BGE into the inter-layer surfaces of octadecyl ammonium modified MMTs (O-MMTs) under ultrasonication, and in a form of liquid nano-reinforcement. It showed advantages of low viscosity, excellent dispersibility and high chemical reactivity in epoxy matrix. The enhancements in tensile and flexural properties of BGE-MMTs/epoxy composites confirmed the well dispersion of BGE-MMTs in epoxy matrix and the strong interfacial adhesion between the two components. More importantly, the well-dispersed BGE-MMTs in epoxy matrix led to significant enhancement in the moisture-barrier properties of epoxy composites. In comparison with that of neat epoxy, the moisture diffusion coefficient of BGE-MMTs/epoxy composites significantly decreased from 10.1×10^{-6} to 0.3×10^{-6} cm^2/s. The enhancement in moisture-barrier properties was ascribed to the exfoliated two-dimensional lamellar structure of MMTs extending the effective penetration paths of water molecules into tortuous forms. A model concerning moisture diffusion in BGE-MMTs/epoxy composites was suggested.

Keywords: montmorillonite; liquid nano-reinforcement; epoxy composite; moisture-resistant.

1. Introduction

Polymer composites have been increasingly used in a variety of fields, due to their advantages of high mechanical strength, good temperature resistance, unique structure-dependent functions and low cost, etc[1-5]. In recent years, epoxy-based composites have been intensely applied in advanced technological fields like separation, storage and transportation of gas and liquid substances with the rapid development of aerospace, aircraft and energy industries. These applications particularly required high barrier capability in addition to excellent mechanical properties. However, epoxy resins had an intrinsic drawback of high moisture absorption and gas permeability that small molecules could permeate, diffuse and transmit into the resin matrix, which in turn deteriorated the barrier functions and mechanical properties of the prepared composites[6-8]. The defects in barrier properties have greatly limited the applications of epoxy-based composites in the aforementioned fields.

It had attracted wide interests in exploiting barrier capability and synchronously enhancing mechanical properties of epoxy-based composites[9-11]. Common approaches included composite technology[12], surface coating technology[13,14] and nanofiller modification technology[15,16], etc. Among them, the addition of functionalized nanofillers was identified as an efficient way to achieve the goal, because the large surface area and the surface functional groups of nanofillers facilitated the formation of uniformly nano-functionalized microstructure in composites even at very low addition amounts. Montmorillonites (MMTs), possessing

unique properties of high strength and large aspect ratio[17,18], were considered as ideal nanofillers for high performance composites. Benefiting from the obstructing function of their two-dimensional nano-layer crystal structure, in particular, MMTs have been identified able to significantly enhance the barrier properties of composites by extending the diffusion and transmission path of small molecules in the resin matrix[15,18]. The reduction of moisture or gas absorption could suppress the internal damage progress and thus obtain long-term performance of composites.

To fully take advantage of MMTs' features in composites, however, the obstacles needed to be overcome were the spontaneously aggregated tactoid layer-structure of MMTs and their distinctively poor interfacial adhesion with polymeric resins[19,20]. It was an essential issue for preparing high performance composites in aspects of barrier and mechanical properties. Chemical functionalization was applied to MMTs, in which, MMTs were exfoliated through chemical modifier intercalating into the inter-layer surface of MMTs[21,22]. The modified MMTs demonstrated strengthened interfacial adhesion and enhanced dispersibility in polymeric resins. For instance, Kim et. al used octadecylamine as organomodifier of MMTs to match the chemical compatibility and the reactivity with epoxy matrix. They found that the addition of such modified MMTs greatly reduced the moisture diffusivity of composites, at the same time, enhanced the thermal and dimensional stabilities[23]. It could be thus deduced that MMTs functionalized with epoxy-type materials should be favorable in producing epoxy-based composites. The epoxy-based modifiers were expected to improve the interfacial adhesion between MMTs and epoxy matrix, not only due to

their chemical compatibility with epoxy matrix, but also due to their reacting ability with the matrix.

Usually, the organically modified MMTs were prepared through complicated treatment process such as filtration, purification and drying, etc[19,20,25], and difficult to be uniformly dispersed in polymer matrixes due to their solid preservation state. In reference to the concept of "carbon nanotube liquid nano-reinforcement" as reported in our previous work[24], herein, a kind of liquid nano-reinforcement containing activated MMTs were proposed and used as nanofillers for epoxy composites. The activated MMTs (BGE-MMTs) were prepared by intercalating butyl glycidyl ether (BGE) into the inter-layer surfaces of octadecyl ammonium modified MMTs (O-MMTs) using one-step ultrasonic treatment. The microstructure and chemical reactivity of BGE-MMTs are suggested in detail in Fig. 1. BGE-MMTs would possess high reacting ability with epoxy matrix as an amine-type curing agent, due to the existence of a reactive -H attached. The liquid nano-reinforcement, in a form of masterbatch, was composed of BGE and uniformly dispersed BGE-MMTs. It showed advantages of reducing processing difficulties in preparing epoxy composites as its viscosity was low. The dispersibility of BGE-MMTs in epoxy composites was systematically evaluated by scanning electron microscope (SEM) and transmission electron microscope (TEM) observations, as well as mechanical property measurements. Then, the moisture-barrier properties of resulting BGE-MMTs/epoxy composites containing various contents of BGE-MMTs were characterized. The moisture diffusivity in epoxy matrix was compared with predicted values by Fick's

second law, and a schematic model was proposed to illustrate the process of moisture diffusion in BGE-MMTs/epoxy composites.

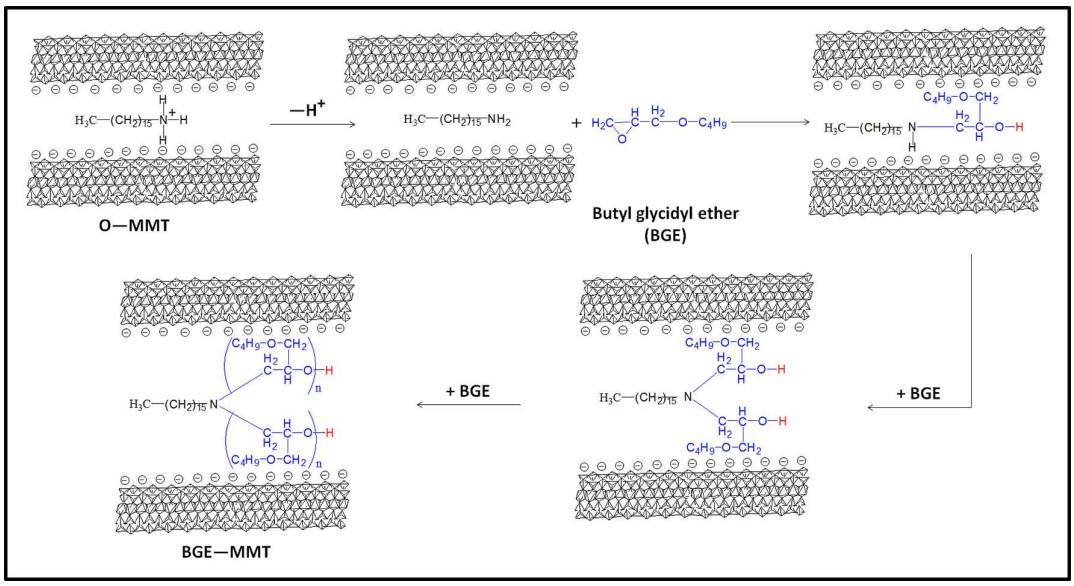

Fig. 1 Schematic preparation of BGE-MMT. The -H marked with red color possesses high chemical reactivity.

2. Experimental section

2.1. Materials

The nanofiller, O-MMTs (octadecyl ammonium 28-32 wt.%, specific gravity 2.8 g/cm^3, average chip thickness < 25 nm), were produced by Zhejiang Fenhong New Material Co., Ltd., China. They were strictly purified by washing with de-ionized water repeatedly to remove any possible impurities before use. BGE was obtained from Aldrich Chemical Co., USA. The resin matrix, diglycidyl ester of aliphatic cyclo (DGEAC) type epoxy, was provided by Tianjin Jindong Chem, China. The hardener, DETDA (74-80 % 3, 5-diethyltoluene-2, 4-diamine and 20-26 % 3, 5-diethyltoluene-2, 6-diamine), was obtained from Lonza, Switzerland. All other chemicals and reagents

were purchased from Beijing Chemical Works (China) and used directly.

2.2. Synthesis of BGE-MMTs

The preparation process of BGE-MMTs is shown in Fig. 1, which was in reference to a similar procedure in our previous work[24]. Briefly, purified O-MMTs were dried in vacuum for 10 h at 90 °C, and then dispersed into BGE with a weight ratio of 1:5 under ice bath. The mixture was subjected to high energy ultrasonic treatment for 1.5 h at 0 °C by applying various powers (200, 400 or 600 W) with a digital sonifier (JY-99Ⅱ, Ningbo Xinzhi Biotechnology Co., Ltd.). To avoid overheating, the ultrasonication was conducted for working 10 s at intervals of 15 s. After the treatment, a kind of masterbatch containing BGE-MMTs was obtained and used as activated liquid nano-reinforcement for epoxy composite preparation.

2.3. Composite preparation

Epoxy mixtures were obtained by uniformly mixing epoxy resin, BGE, BGE-MMTs containing masterbatch and other agents under ultrasonic treatment in reference to our previous works[26-28]. The BGE-MMTs/epoxy composites were prepared by pouring epoxy mixtures into molds and curing at 80 °C /1 h + 100 °C /1 h + 120 °C /3 h. For controlling the uniformity of the obtained BGE-MMTs/epoxy composites, the gelation time of epoxy matrix was adjusted to be around 0.5 h. The weight ratio of epoxy, BGE, hardener and accelerator was 70:30:30:3 in the composites, and the content of BGE-MMTs was adjusted to be 0, 1, 2, 3, 4 or 5 wt.% of the total weight of epoxy and BGE.

2.4. Characterizations

Surface functional groups on both pristine O-MMTs and BGE-MMTs were detected with Fourier transform infra-red spectroscope (FT-IR, Nexus670, Nicolet). Element analysis was conducted on X-ray photoelectron spectroscope (XPS, ESCALAB 250, Thermo Scientific) using monochromatised AlKα X-ray source at a constant analyzer. Loading contents of BGE onto O-MMTs were measured on thermogravimetric analyzer (TGA, Q500, TA) at a heating rate of 10 °C/min from 35 to 900 °C under nitrogen atmosphere. Morphological observations were performed on both SEM (S4700, Hitachi) and transmission electron microscope TEM (JEM100CX, Leica). Before SEM examination, specimens were coated with a thin layer of a gold alloy. For TEM measurement, specimens were embedded directly in Spurr resin before sectioning at room temperature on Ultracut UCT microtome (Leica-Vienne). Ultrathin sections were collected on formvar carbon coated 100 mesh nickel grids.

Tensile and flexural properties of epoxy composites were measured by mechanical testing machine (INSTRON 1121) according to ASTM D 638 and ASTM D 790, respectively. All final values of tensile and flexural properties were averages of five measurements. Dynamic mechanical thermal analysis (DMTA) of epoxy composites was performed using a TA instrument (Q800, TA) at a heating rate of 5 °C/min from 35 to 200 °C. The glass transition temperature (T_g) was measured from the peak of the *Tanδ* spectrum.

The moisture-barrier properties of epoxy composites were tested on an experimental setup as illustrated in Fig. 2. Moisture absorption of one-dimensional diffusion mode was preferred, therefore, thin plate with two parallel planes was used

for the test by measuring the weight change with moisture absorption. Briefly, circular specimens, with 25 mm in diameter and 1.5 mm in thickness, were dried in an oven at 80 °C for 24 h to remove any hint of moisture before the testing. Subsequently, the specimens were tightly fixed with two silicone circles consisting of sealed fences. The upper surface of the specimen was exposed to an environment of 99 % RH at 90 °C. The lower surface of the specimen was faced to a vacuum environment. The specimens were retrieved from the test chamber at intervals of 12 h, and weighed using Mettler Toledo balance with accuracy of 0.00001 g for decreasing the experimental error. The weight gain fractions of the resin specimens $\omega(t)$ were calculated by Eq. (1):

$$\omega(t) = \frac{m_t - m_0}{m_0} \times 100 \quad (1)$$

Where m_t is the time-varying weight of specimens and m_0 is the initial weight. For decreasing the experimental error, all final values of weight gain fractions $\omega(t)$ were averages of five measurements.

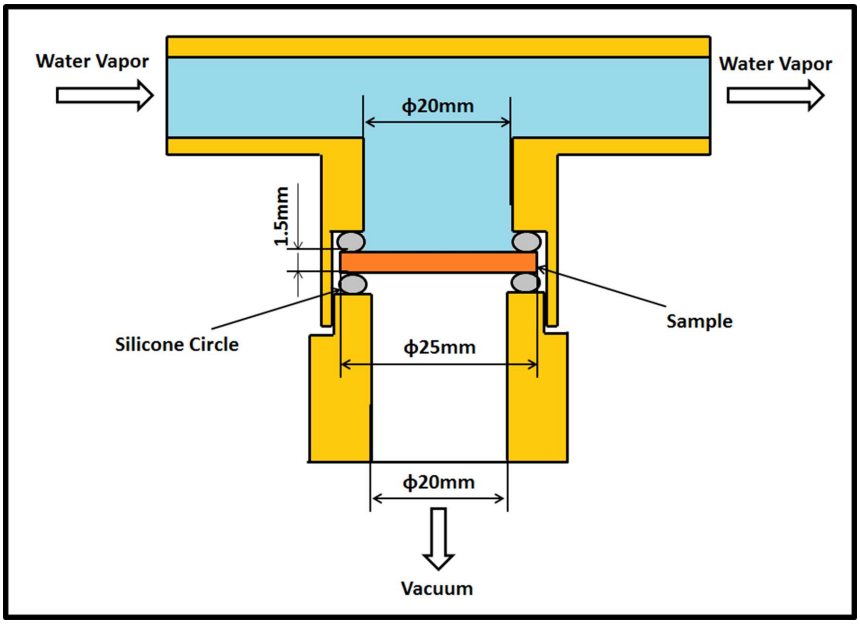

Fig. 2 Experimental setup of the moisture barrier test.

2.5. Evaluation of moisture diffusion in polymeric materials

Moisture diffusion in resin could be described by the Fick's second law as a non-steady state diffusion using Eq. (2)[23]:

$$\frac{\partial c}{\partial t} = D\left(\frac{\partial^2 c}{\partial x^2} + \frac{\partial^2 c}{\partial y^2} + \frac{\partial^2 c}{\partial z^2}\right) \quad (2)$$

where c is the concentration of diffusing substance, t is time, D is the diffusion coefficient, and x, y, z denote the coordinate location.

For one-dimensional diffusion through a plate with two parallel planes, Eq. (2) could be reduced to Eq. (3):

$$\frac{\partial c}{\partial t} = D\frac{\partial^2 c}{\partial x^2} \quad (3)$$

The total weight gain fraction of the resin specimen could be obtained by integrating the solution of Eq. (3) using the straight diffusion length of moisture based

on Eq. (4)[29, 30]:

$$\omega(t) = \omega_\infty - 2\frac{(\omega_\infty - \omega_0)}{\pi^2}\sum_{i=1}^{\infty}\frac{\left(1-(-1)^i\right)^2}{i^2}\exp\left[-(\pi i/s)^2 Dt\right] \quad (4)$$

where ω_∞ is the equilibrium moisture content and ω_0 is the initial moisture content in specimen, as well as s is the straight diffusion length of moisture, which could be considered to be the initial thickness of resin specimen.

By assuming that the initial moisture content in resin specimen $\omega_0 = 0$ and for large value of time $i = 1$, Eq. (4) could be reduced to Eq. (5):

$$\omega(t) = \omega_\infty - 8\frac{\omega_\infty}{\pi^2}\exp\left[-(\pi/s)^2 Dt\right] \quad (5)$$

The rate of moisture absorption could be calculated by the time derivative of moisture content in Eq. (5), which was determined by Eq. (6):

$$\frac{d\omega}{dt} = 8\frac{\omega_\infty D}{s^2}\exp\left[-(\pi/s)^2 Dt\right] \quad (6)$$

Further obtaining $8\omega_\infty \exp\left[-(\pi/s)^2 Dt\right] = (\omega_\infty - \omega(t))\pi^2$ from Eq. (5) and substituting it in Eq. (6), which resulted in Eq. (7) for evaluation the rate of moisture absorption:

$$\frac{d\omega}{dt} = \frac{\pi^2 D}{s^2}(\omega_\infty - \omega(t)) \quad (7)$$

Since $\frac{d\omega}{dt}$ was linearly dependent on $\omega(t)$ and the interception point with ω axis corresponded to equilibrium moisture content ω_∞, therefore, the inclination angle of the curve of Eq. (7) determined the diffusion coefficient D, which was obtained by Eq. (8):

$$D = -\frac{s^2}{\pi^2}\frac{\Delta\frac{d\omega}{dt}}{\Delta\omega} \quad (8)$$

The diffusion coefficient D of resin specimen obtained by Eq. (8) was independent on relative humidity of atmosphere.

2.6. Evaluation of mechanical properties of composites by modeling

The well-established Halpin Tsai theory (HTT) for one-dimensional nanoparticles reinforced composites was utilized to predict the Young's modulus of the nanocomposites[31]. To model the elastic modulus of epoxy composites reinforced with BGE-MMTs, each BGE-MMT platelet was considered acting as an effective rectangular solid fiber with length (t), width (d) and thickness (h) in this study. Accordingly, the HTT equation was modified as expressed as Eq. (9)[31,32]:

$$E_{MMT/EP} = \frac{3}{8}\times\frac{1+\left[\left(t+d\right)/h\right]\frac{\left(E_{MMT}/E_{EP}\right)-1}{\left(E_{MMT}/E_{EP}\right)+\left(t+d\right)/h}V_{MMT}}{1-\frac{\left(E_{MMT}/E_{EP}\right)-1}{\left(E_{MMT}/E_{EP}\right)+\left(t+d\right)/h}V_{MMT}}\times E_{EP} + \frac{5}{8}\times\frac{1+2\frac{\left(E_{MMT}/E_{EP}\right)-1}{\left(E_{MMT}/E_{EP}\right)+2}V_{MMT}}{1-\frac{\left(E_{MMT}/E_{EP}\right)-1}{\left(E_{MMT}/E_{EP}\right)+2}V_{MMT}}\times E_{EP} \quad (9)$$

where $E_{MMT/EP}$, E_{MMT} and E_{EP} denote the Young's modulus of epoxy composites with BGE-MMTs, BGE-MMTs themselves and pure epoxy matrix, respectively, as well as V_{MMT} represents the volume fraction of BGE-MMTs in epoxy composites. In this study, the estimated E_{MMT} and E_{EP} of 360 and 2.3 GPa[33,34], respectively, were used in the calculation, associated with the measured t, d and h of 20 μm, 15 μm and 10 nm. The density of BGE-MMTs (ρ_{MMT}) was estimated to be ~2.8 g/cm^3[35,36], and the density of

epoxy matrix (ρ_{EP}) was determined to be ~1.2 g/cm^3[26]. Herein, V_{MMT} could be calculated based on Eq. (10) and (11):

$$\rho_{MMT/EP} = \rho_{MMT}V_{MMT} + \rho_{EP}(1 - V_{MMT}) \quad (10)$$

$$V_{MMT} = \frac{\rho_{MMT/EP}}{\rho_{MMT}} W_{MMT} = \frac{W_{MMT}}{W_{MMT} + (\rho_{MMT}/\rho_{EP})(1 - W_{MMT})} \quad (11)$$

where W_{MMT} is the weight fraction of BGE-MMTs in epoxy composites and $\rho_{MMT/EP}$ is the density of the composite reinforced with BGE-MMTs.

3. Results and discussion

3.1. Characterization of BGE-MMTs

The prepared BGE-MMTs were investigated with characterizations of FT-IR, XPS and TGA. As shown in Fig. 3, the strong absorption peaks at 3181 and 3251 cm^{-1} in the FT-IR spectrum of O-MMTs were originated from characteristic N-H stretching vibration of -NH_2 group from octadecyl surface modifier. Compared to the original O-MMTs, these two peaks disappeared in the spectra of all BGE-MMTs specimens treated with various ultrasonic powers, indicating the changes of functional groups on the surface of MMTs due to the reaction between -NH_2 group of O-MMTs and epoxide group of BGE as shown in Fig. 1. Changes in surface elements of BGE-MMTs were confirmed by XPS data. In Fig. 4(a), O-MMTs displayed binding energies of C_{1s} at 284.9 eV and N_{1s} at 402.5 eV, which were assigned to the carbon chain and the -NH_3^+ of octadecyl ammonium modifiers, respectively. The element peaks of O_{1s} at 531.4, 532.2 and 532.8 eV were attributed to Al-O, Si-O and -OH in O-MMTs. In the XPS spectra of

BGE-MMTs as shown in Fig. 4(b), in addition to the aforementioned peaks of C_{1s}, N_{1s} and O_{1s}, an extra peak of O_{1s} at 533.6 eV was detected, which was attributed to the $-CH_2-O-C_4H_9$ from BGE component. Additionally, the C/N atomic ratio calculated from the XPS spectrum of O-MMTs was 15.7, while the C/N atomic ratio of BGE-MMTs increased to be 18.1 when the treating power was 600 W. The excess carbon atoms apparently came from the grafted BGE onto O-MMTs. These facts clearly confirmed the successful grafting of BGE onto the surface of O-MMTs.

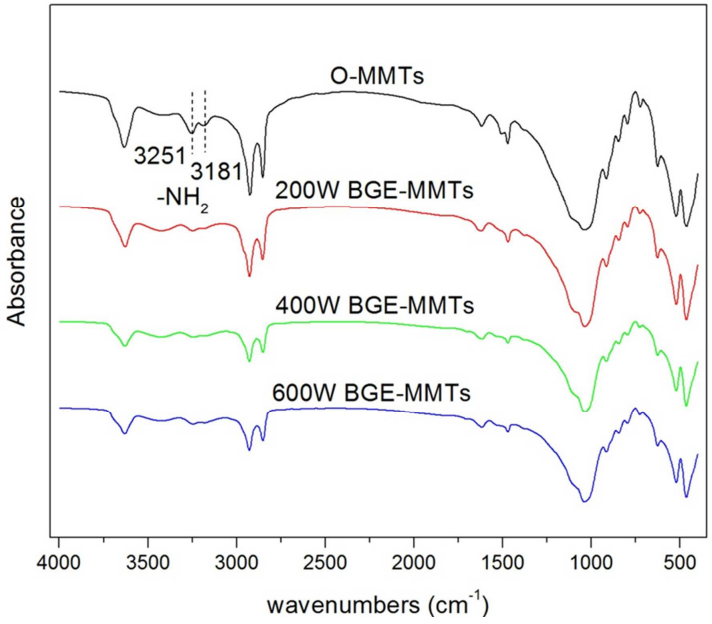

Fig. 3 FT-IR spectra of O-MMTs and BGE-MMTs treated under various ultrasonic powers.

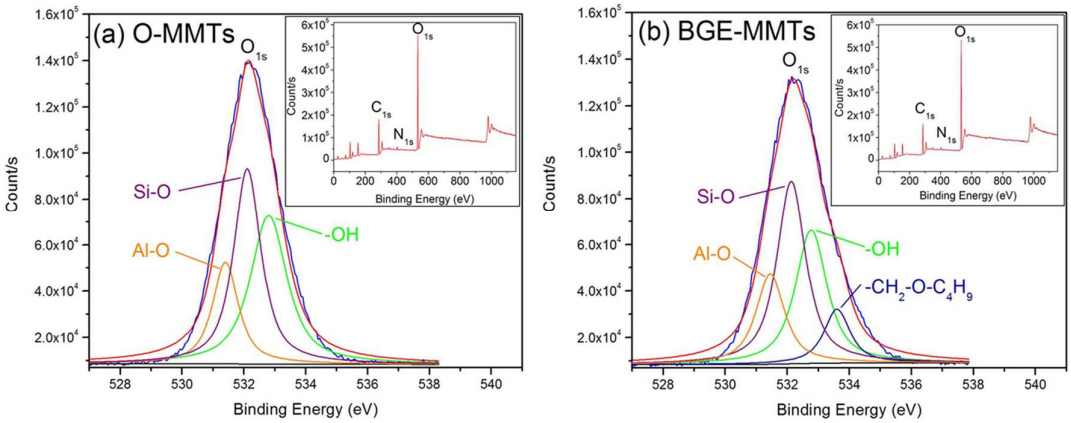

Fig. 4 Survey XPS spectra of O_{1s} for (a) O-MMTs and (b) BGE-MMTs treated under ultrasonic power of 600 W. The insets are the corresponding XPS spectra.

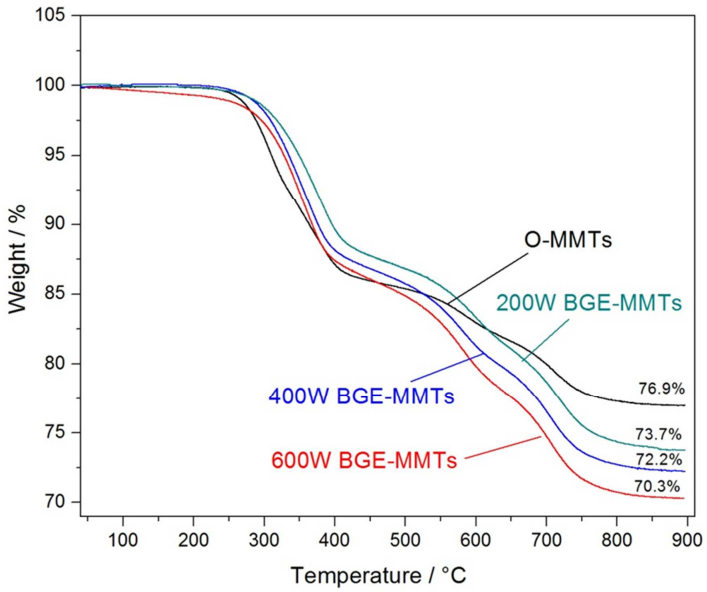

Fig. 5 TGA curves of O-MMTs and BGE-MMTs treated under various ultrasonic powers.

Fig. 5 shows the TGA curves of O-MMTs and BGE-MMTs treated with various ultrasonic powers. It was found that the weight loss fractions of O-MMTs and BGE-MMTs treated with ultrasonic powers of 200, 400, 600 W were 23.1, 26.3, 27.8

and 29.7 wt.%, respectively. The weight loss fractions of all BGE-MMTs were higher than that of O-MMTs, and the values increased with the treating power increasing. In comparison with O-MMTs, the higher weight loss of BGE-MMTs came from the decomposition of the grafted BGE. The weight fraction of grafted BGE could be calculated from TGA data using the equation of $f_{O\text{-}MMTs}=(1\text{-}X)\times f_{BGE\text{-}MMTs}$, where $f_{O\text{-}MMTs}$ and $f_{BGE\text{-}MMTs}$ are the weight loss fraction of O-MMTs and BGE-MMTs, respectively, and X denotes the weight fraction of BGE in BGE-MMTs[37]. The calculated weight fractions of BGE in BGE-MMTs were 12.2, 17.0 and 22.2 wt.%, respectively, when the treating ultrasonic powers were 200, 400 and 600 W. More BGE component had been grafted onto MMTs by increasing the ultrasonic power, and ultrasonic treatment could apparently enhance the reactions between O-MMTs and BGE.

3.2. Analysis of BGE-MMTs dispersion in epoxy composites

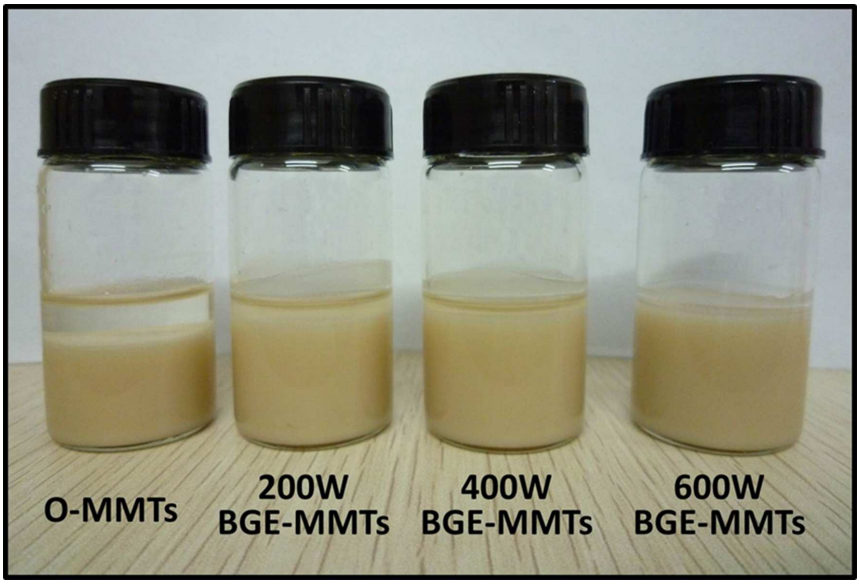

Fig. 6 Optical images of O-MMTs dispersed in BGE without and with ultrasonic treatment under various powers followed by standing for 24 hours.

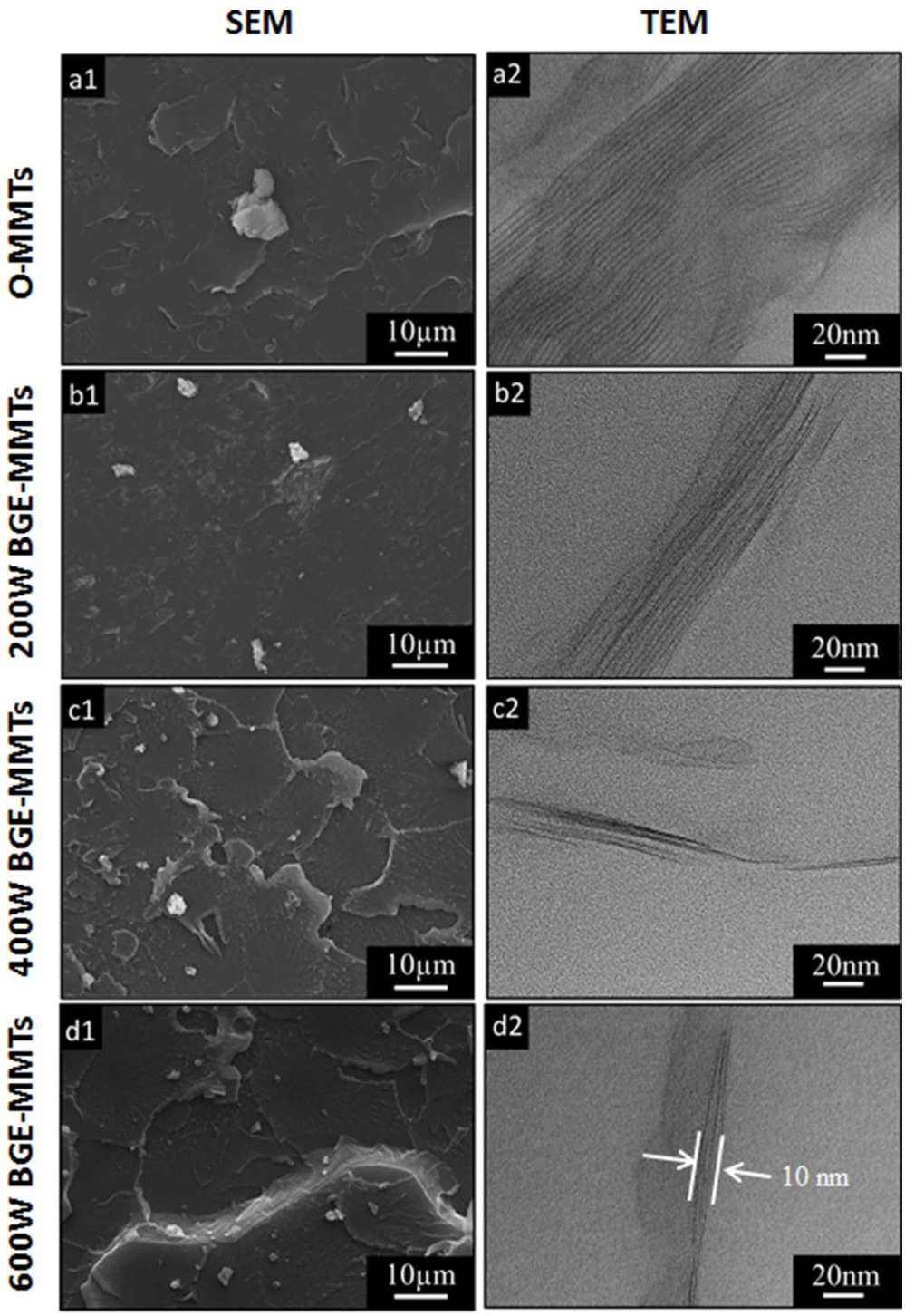

Fig. 7 SEM and TEM images of fractured surfaces of epoxy composites with 1 wt.% O-MMTs (a1, a2) and 1 wt.% BGE-MMTs treated under ultrasonic powers of (b1, b2) 200 W, (c1, c2) 400 W, (d1, d2) 600 W.

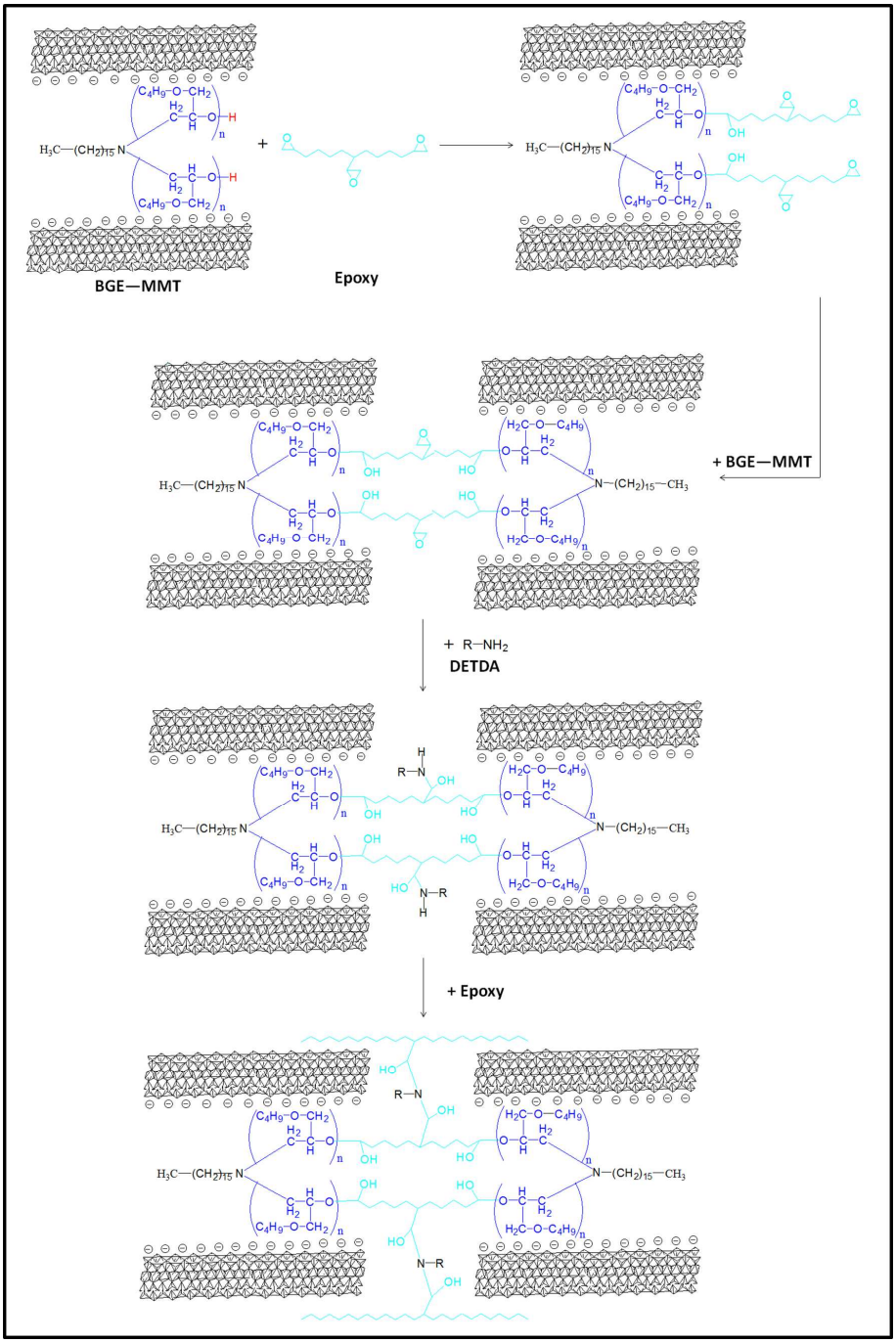

Fig. 8 Schematic of the interfacial reaction between BGE-MMTs and epoxy matrix. The reactive -H as marked with red color can open the epoxy ring of an epoxy resin as an amine-type curing agent and finally generate the three-dimensional crosslinked structure at the interfacial region between BGE-MMTs and epoxy matrix.

To investigate the effect of BGE grafting on the dispersibility of MMTs, optical images of the prepared masterbatch of O-MMTs or different BGE-MMTs suspending in BGE were taken after standing for 24 h. As shown in Fig. 6, O-MMTs could be seen subsiding to the bottle bottom, showing their poor dispersion in BGE. In contrast, the BGE-MMTs showed perfect and stable dispersion in BGE without any optical phase separation over time, when the treating power was 600 W. In cases of BGE-MMTs obtained from ultrasonication of 200 and 400 W, however, the occurrence of slight phase separation was still observed. It was obvious that the dispersion of BGE-MMTs in epoxy could be greatly enhanced by raising the grafting content of BGE via increasing ultrasonic power.

Epoxy composites containing 1 wt.% of different MMTs were then prepared as mentioned in the experimental section, and morphologies of fractured surfaces were observed by SEM and TEM (Fig. 7). From Fig. 7(a1), O-MMTs were found existing in the form of serious aggregation in the epoxy matrix. In Fig. 7(a2), O-MMTs showed the presence of tactoids of big thickness. They displayed clear multi-lamellar structure, which was composed of non-exfoliated platelets. On the contrary, BGE-MMTs dispersed more uniformly in epoxy composites with better interfacial adhesion (Fig. 7(b1,c1,d1)). TEM images of BGE-MMTs revealed their typical exfoliated lamellar structure (Fig. 7(b2,c2,d2)). The well-exfoliated BGE-MMT layers exhibited platelet-like shape due to their large aspect ratio. The aggregation of BGE-MMTs was decreased as the treating ultrasonic power increasing, and the dispersion degree in

epoxy composites was improved accordingly. Among the three BGE-MMTs, BGE-MMTs treated with ultrasonic power of 600 W showed the best dispersion in epoxy matrix as a result of the high grafting content of BGE and the resulting excellent exfoliation of lamellar structure. Therefore, BGE-MMTs treated with ultrasonic power of 600 W were selected as highly effective nano-reinforcements in the following parts of this study.

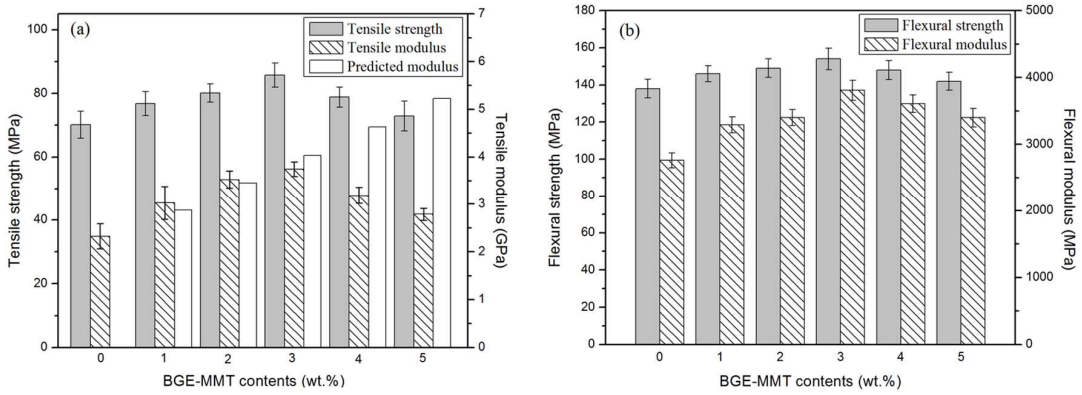

Fig. 9 (a) Tensile and (b) flexural strength and modulus of epoxy composites with various contents of BGE-MMTs treated under ultrasonic power of 600 W.

As reported in literatures[38-41], MMTs were usually used as effective nano-reinforcements in polymeric composites due to their high mechanical properties. The chemically strengthened interfacial adhesion between BGE-MMTs and epoxy matrix would further make BGE-MMTs effective reinforcements for epoxy composites. As shown in Fig. 1 and Fig. 8, the existence of a reactive -H attached in BGE-MMTs could open the epoxy ring of an epoxy resin and act as an amine-type curing agent. The reaction characteristics would make MMTs being involved into the cross-linking reaction of the epoxy during thermal curing. As a result, the mechanical properties of

BGE-MMTs/epoxy composites should be significantly enhanced.

Theoretically, the enhancement in mechanical strength and modulus of BGE-MMTs/epoxy composites should be kept going up continuously with the content of BGE-MMTs increasing (Fig. 9). As shown in Fig. 9(a), the theoretical Young's modulus for epoxy composites with various contents of BGE-MMTs were predicted based on HTT model, which distinctly displayed an ascending trend with the content of BGE-MMTs. However, the practical reinforcing effect closely related to the dispersion state of MMTs in composites. The maximum tensile strength and modulus of BGE-MMTs/epoxy composites were obtained with the addition of 3 wt.% of BGE-MMTs, which was inconsistent with the predicted values at higher content of BGE-MMTs (Fig. 9(a)). Similar trend was detected in flexural properties of BGE-MMTs/epoxy composites (Fig. 9(b)). Compared to the neat epoxy the improvement in the tensile and flexural properties of BGE-MMTs/epoxy composites manifested the reinforcing effect of BGE-MMTs, as the content of BGE-MMTs increasing from 0 to 3 wt.%. In these cases, the well-exfoliated BGE-MMT layers could be seen dispersed uniformly in epoxy as confirmed by SEM and TEM observations (Fig. 10(a1-a2), (b1-b2) and (c1-c2)), which accounted for the enhancement in mechanical properties. As the content of BGE-MMTs was further increased above 3 wt.%, aggregation of nano-scaled BGE-MMTs was clearly detected (Fig. 10(d1-d2) and (e1-e2)). MMTs could be seen stacking together, and insufficient impregnation of epoxy resin into BGE-MMT platelets would occur, and thus the structural defects in the

composites were generated accordingly. Although the 600 W treated BGE-MMTs had shown good dispersion in epoxy composites, it was hard to avoid aggregation of nanofillers when the content was high as reported in many literatures[42,43]. During mechanical property evaluation, these defects resulted in the great stress concentration and easy crack propagation in the matrix, leading to the subsequent decrease in mechanical strength and modulus.

The reinforcing effect of BGE-MMTs on epoxy composites was also evaluated by DMTA. As shown in Fig. 11(a), the storage moduli (E') of BGE-MMTs/epoxy composites were apparently higher than that of neat epoxy. With the content of BGE-MMTs increasing, the E' of composite was remarkably enhanced, indicating the steady enhancement in the stiffness of the composite. From Fig. 11(b), the glass transition temperatures (T_g) of epoxy composites were also found increasing with higher content of BGE-MMTs. This phenomenon was consistent with many reported data focusing on reinforcing effects of nano-scaled fillers[41,44-46]. The T_g of polymer matrix was suggested depending on the free volume of the polymer, which closely related to the affinity between the filler and the polymer matrix[41]. Since BGE-MMTs possessed chemical reactivity with epoxy resin and excellent compatibility with molecular chains of epoxy matrix, the presence of BGE-MMT platelets would confine the movement of molecular chains of epoxy matrix and thus reduce the free volume of epoxy matrix. Therefore, the T_g of BGE-MMTs/epoxy composite moved to higher temperature as a result of the restricted molecular chain movement. More BGE-MMTs were incorporated,

epoxy composites with higher thermal stability were obtained.

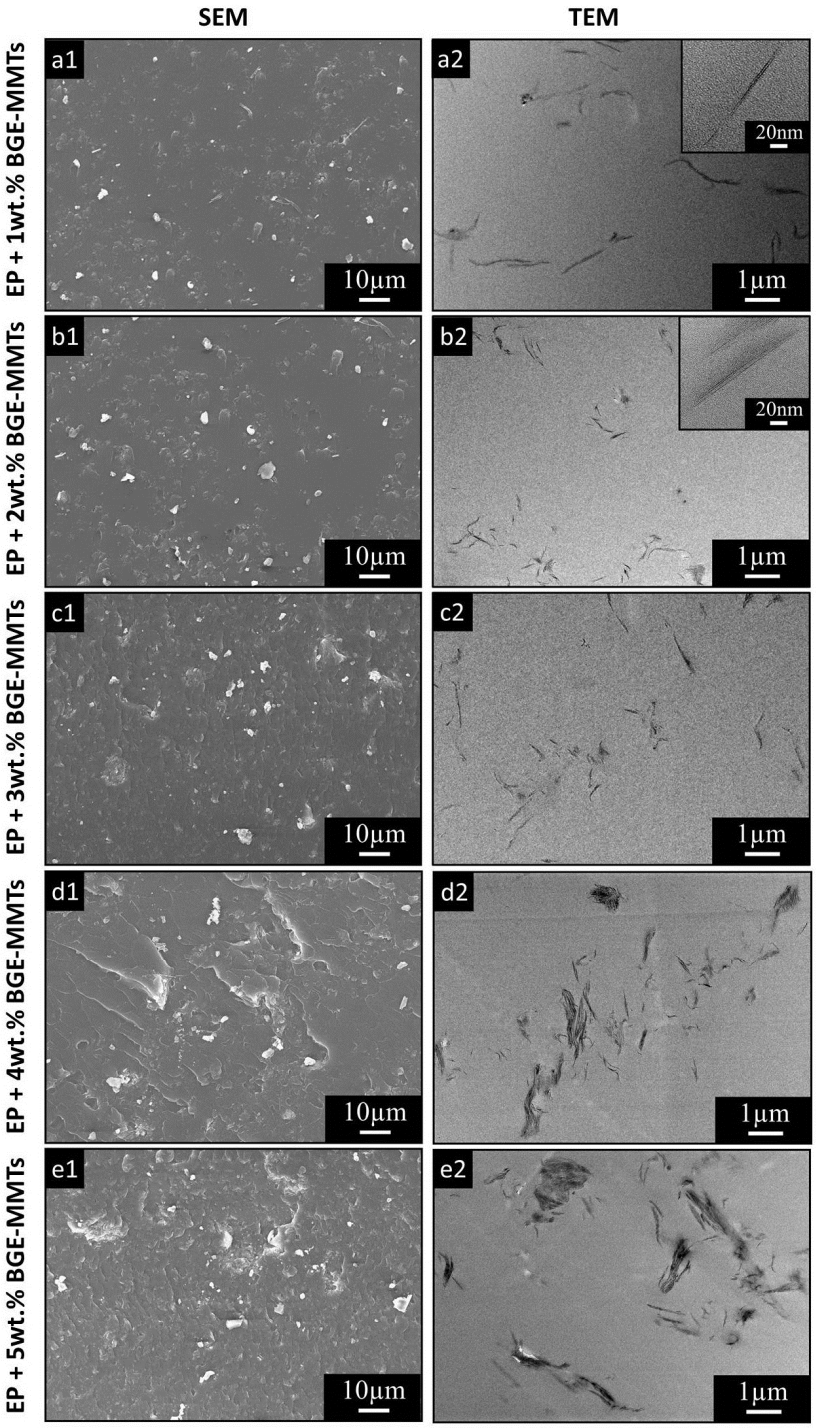

Fig. 10 SEM and TEM images of fractured surfaces of epoxy composites with various contents of BGE-MMTs treated under ultrasonic power of 600 W: (a1, a2) 1 wt.%, (b1,

b2) 2 wt.%, (c1, c2) 3 wt.%, (d1, d2) 4 wt.%, (e1, e2) 5 wt.%.

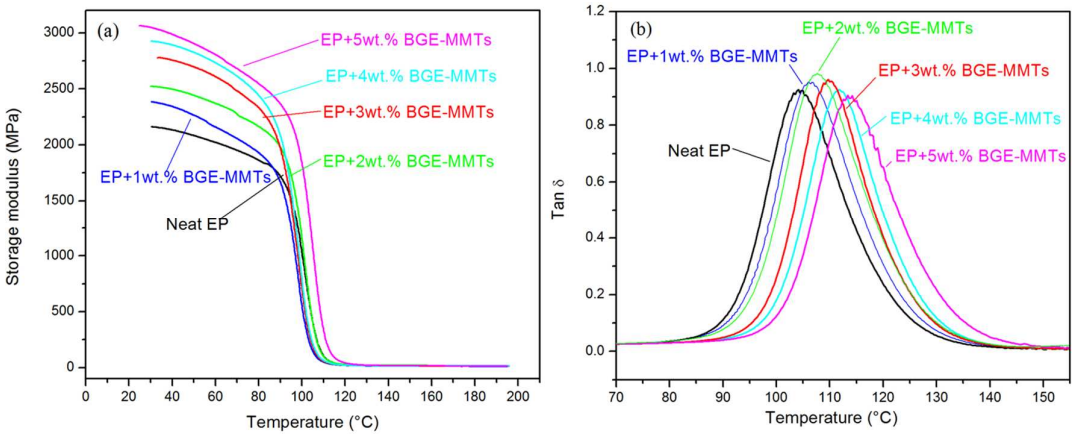

Fig. 11 (a) Storage modulus and (b) Tanδ of epoxy composites with various contents of BGE-MMTs treated under ultrasonic power of 600 W.

3.3. Evaluation of moisture diffusion in BGE-MMTs/epoxy composites

BGE-MMTs/epoxy composites containing different contents of BGE-MMTs were submitted to the study of moisture barrier properties as described in the experimental section. Plots of weight gain fraction versus time per specimen square thickness are shown in Fig. 12. Those solid lines presented in Fig. 12 were the predicted curves based on the Fick's second law by using Eq. (5). It was found that the experimental moisture absorption behavior of epoxy composites fitted well with the Fick's second law. For all epoxy composites, the weight gain increased at the initial stage and then the moisture saturation was achieved gradually. For the neat epoxy, the weight gain showed an explosive increasing trend initially and leveled off within short time. With the addition of BGE-MMTs, however, the rate of weight gain was distinctively reduced.

BGE-MMTs/epoxy composites needed longer time to reach moisture saturation, especially for BGE-MMTs/epoxy composites containing higher content of BGE-MMTs. Besides, the weight gaining also went down as the content of BGE-MMTs increasing. When the content of BGE-MMTs was 5 wt.%, the rate of weight gain was quite slow, where the weight gain fraction was below 5 wt.%.

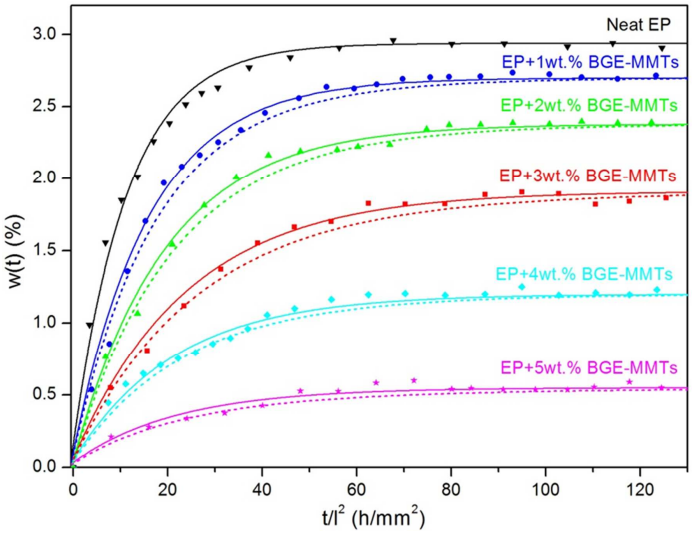

Fig. 12 Plots of weight gain fraction w(t) (%) versus time (h) per specimen square thickness (mm), t/l^2 (h/mm^2), for epoxy composites with various contents of BGE-MMTs treated under ultrasonic power of 600 W. The solid lines show the prediction curves based on the Fick's second law. The dotted lines show the prediction curves based on the Langmuirian solution.

The differences in moisture absorption behaviors were suggested due to the barrier effect of exfoliated BGE-MMTs, whose two-dimensional lamellar structure were able to block the diffusion of water molecules in epoxy matrix. When the exfoliated BGE-MMTs were uniformed dispersed in the matrix, their two-dimensional lamellar

structure with large aspect ratio would extend the effective penetration path of small molecules, and thus reduce the diffusion coefficient of small molecules. It could be envisioned that such effect would be enhanced by increasing the content of BGE-MMTs. Based on the Fick's second law, the moisture diffusivity data for BGE-MMTs/epoxy composites were calculated and shown in Fig. 13. The descending curve along the content of BGE-MMTs confirmed that the diffusion of water molecules in BGE-MMTs/epoxy composites proceeded much more slowly than in neat epoxy. Compared with that of neat epoxy, the average diffusion coefficient $<D>$ of epoxy composites with 3 wt.% BGE-MMTs was decreased as much as 96.6% from 10.1×10^{-6} to 0.3×10^{-6} cm^2/s. Though the diffusivity demonstrated a reverse correlation to the content of BGE-MMTs, the diffusion coefficient did not decrease further as expected when the content of BGE-MMTs was higher than 3 wt.%. The phenomenon should be related to the dispersion state of BGE-MMTs. As shown in Fig.10, aggregations of BGE-MMTs were visible when the content of BGE-MMTs was higher than 3 wt.%. MMTs stacked together and their barrier effect was not as effective as that of well-dispersed MMTs. Therefore, the moisture diffusion coefficient of BGE-MMTs/epoxy composites leveled off as the content of BGE-MMTs being further increased.

Based on all these results and analysis, the function of BGE-MMTs in epoxy composites and the barrier mechanism of BGE-MMTs/epoxy composites were proposed and illustrated in Fig. 14. The process of moisture diffusion in BGE-MMTs/epoxy

composites could be divided into three stages. In the initial stage, water molecules tended to go into the voids or defects of the epoxy matrix from the surface facing to saturated moisture, and then spread inside the matrix randomly as a function of Brown motion. If the composites did not contain BGE-MMT platelets, the water molecule (Label I) could directly go through the epoxy matrix by finishing numerous penetration sub-paths (P_{mk}). The presence of BGE-MMTs in the epoxy matrix would change the diffusion process of water molecules into the tortuous path, since water molecules could not penetrate the BGE-MMT platelets. Thus, the intermediate stage was that BGE-MMTs greatly extended the effective penetration path of water molecules by producing numerous additional sub-paths (P_{bk}) around BGE-MMTs platelets. In this way, the total penetration path length of water molecules was the sum of all sub-paths (P_{mk}) through the matrix and all sub-paths (P_{bk}) around BGE-MMTs. It cost much more time for water molecules to pass by the nanofillers due to the great extension of diffusion path. Therefore, the moisture diffusion coefficient of BGE-MMTs/epoxy composites obviously decreased in comparison with that of neat epoxy matrix. In the final stage, water molecules had gone through the entire diffusion path and would diffuse out of the matrix from the other side of specimens. However, it should be noted that the functional structure of epoxy composites based on BGE-MMTs would directly influence the moisture diffusion coefficient in the composites. Ideally, if the layers of BGE-MMTs distributed parrallel to the surface of specimen and vertical to the diffusion direction of water molecules at the same time, the moisture diffusion coefficient in

epoxy composites was the smallest due to the greatest extension of water molecule diffusion path by the nanofillers. On the contrary, if the layers of BGE-MMTs distributed parrallel to the diffusion direction of water molecules, the moisture diffusion coefficient in epoxy composites was the biggest. Therefore, the moisture diffusion coefficient measured in this study should locate between those values of aforementioned two cases due to the random distribution of BGE-MMTs.

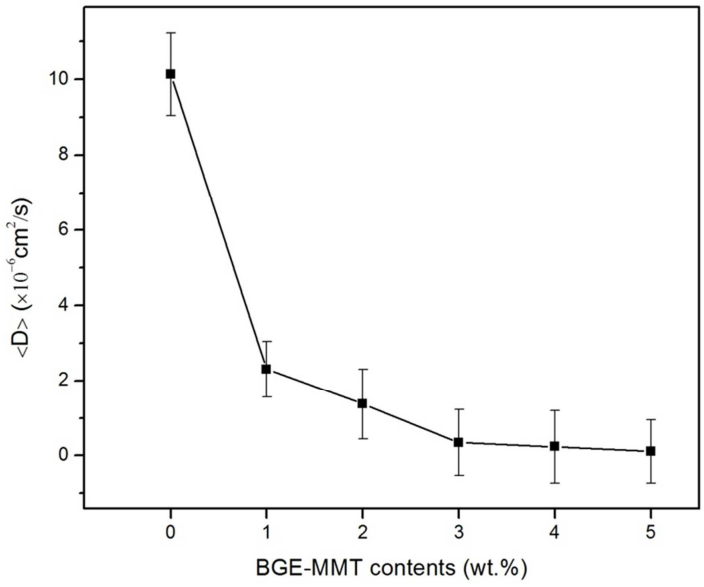

Fig. 13 Variation of moisture diffusion coefficient as a function of BGE-MMT (treated under 600 W) content for epoxy composites.

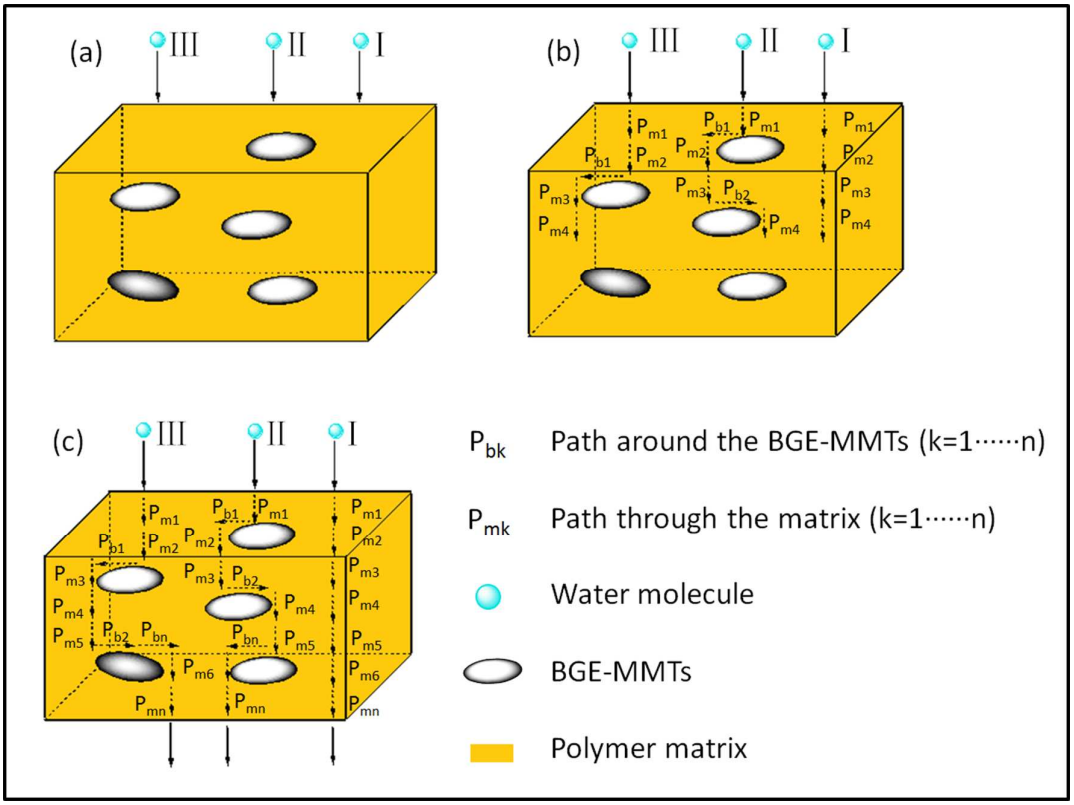

Fig. 14 Schematic model of moisture diffusion in BGE-MMTs/epoxy composites at (a) initial stage, (b) intermediate stage and (c) final stage.

Calculation on relative diffusion path was thought helpful in elucidating the barrier effect of BGE-MMTs on moisture diffusion in epoxy composites. The diffusion path for those water molecules directly going through the epoxy matrix could be expressed as Eq. (12). And the diffusion path for water molecules meeting with BGE-MMTs platelets could be expressed as Eq. (13). In this case, the moisture content could be expressed using one-dimensional Langmuirian solution having two exponential terms based on Eq. (14)[23]:

$$I_0 = \sum_{k=1}^{n} P_{mk} \qquad (12)$$

$$l = \sum_{k=1}^{n} \left(P_{mk} + P_{bk} \right) \tag{13}$$

$$\omega(t) = \omega_{\infty} - \frac{v}{u+v} \omega_{\infty} exp(-ut) - \frac{u}{u+v} 8 \frac{\omega_{\infty}}{\pi^2} exp\left[-(\pi/l)^2 Dt \right] \tag{14}$$

where u and v are positive constants representing two phases of a free diffusible phase and an indiffusible trapped phase, respectively. The approximate values $\frac{v}{u+v}$ could be obtained from the first plateau of the moisture absorption curve shown in Fig. 12. The calculated curves based on the one-dimensional Langmuirian solution in Eq. (14) were superimposed as the dotted lines in Fig. 12, which matched well with the practical moisture adsorption curves.

The relationship between l_0 and D for moisture adsorption was known as Eq. (15)[23]:

$$l_0 = \pi \sqrt{\frac{D}{u}} \tag{15}$$

The total path l for moisture through the matrix and around the BGE-MMTs could be calculated from Langmuirian prediction curves, and the relative diffusion paths l/l_0 versus BGE-MMT content in epoxy composites were plotted in Fig. 15. It could be clearly seen that the values of l/l_0 were substantially increased with higher BGE-MMT content. And the increment of l/l_0 became insignificant when BGE-MMT content was above 3 wt.%. The calculations displayed consistent results as those shown in Fig. 12 and Fig. 13. Both experimental data and theoretical analysis confirmed that well-dispersed BGE-MMT platelets in epoxy matrix were effective nanofillers to enhance the barrier properties of epoxy composites.

In a word, such highly moisture-resistant epoxy composites could be used to explore high-performance composite container products for separation, storage and transportation of gas and liquid substances in advanced technological fields of aerospace, aircraft and energy industries, etc. Moreover, the one-step reaction approach, which was used to prepare the activated liquid nano-reinforcement containing MMTs in this study, could be extended to prepare a variety of high performance polymer composites functionalized with other liquid nano-reinforcements containing nanofillers like carbon nanotubes, carbon nanofibers and graphenes, etc..

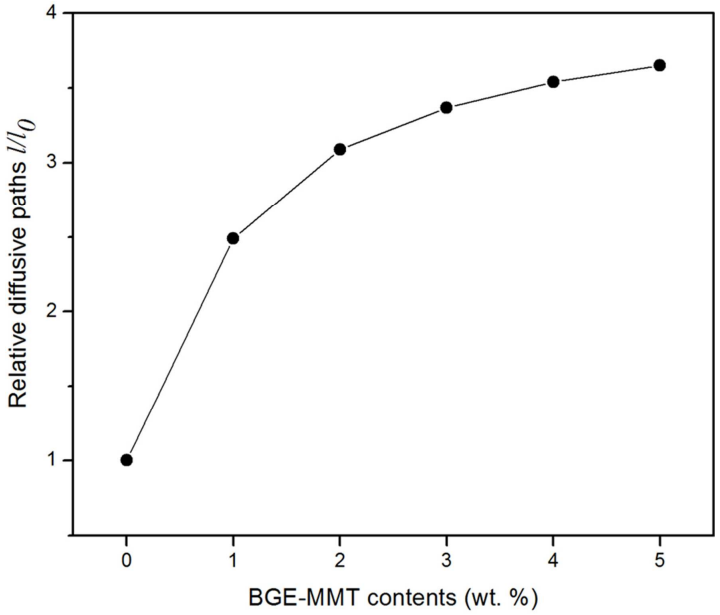

Fig. 15 The curve for the relative diffusion paths l/l_0 versus BGE-MMT content in epoxy composites.

4. Conclusions

Chemical functionalization of nano-scaled O-MMTs with reactive BGE under ultrasonication was proven a facile and efficient way to prepare BGE-MMTs, and a kind of

activated MMT liquid nano-reinforcement was readily obtained. By raising the treating power of ultrasonication, the dispersion and interfacial adhesion of BGE-MMTs in epoxy composites were substantially improved due to the increasing in both the grafting content of BGE onto MMTs and the exfoliation degree of MMTs. Benefiting from the well-dispersion of BGE-MMTs in epoxy matrix and the chemically strengthened interfacial adhesion between them, the moisture-barrier properties of BGE-MMTs/epoxy composites were significantly enhanced. The mechanism of the addition of BGE-MMTs able to enhance the moisture-barrier properties was proposed that their two-dimensional lamellar structure of MMTs obstructed the direct penetration of water molecules, and the effective penetration path of water molecules in composites was largely increased by circumventing MMTs. In conclusion, the liquid nano-reinforcement containing well-dispersed activated BGE-MMTs was easily mixed with epoxy resin, and effective in producing composites with enhanced barrier and mechanical properties for exploring high-performance container products for separation, storage and transportation of gas and liquid substances in advanced technological fields of aerospace, aircraft and energy industries, etc.

Acknowledgement

The authors are very pleased to acknowledge financial support from the National Natural Science Foundation of China (Grant No. U1362205, 5157031049, 51373016), Natural Science Foundation of Jiangsu Province (Grant No. SBK2014040489), National High Technology Research and Development Program of China (Grant No. 2012AA03A203), Beijing Youth Talent Plan (Grant No. YETP0492) and 2014 Open Project of State Key

Laboratory of Organic-Inorganic Composites.

Notes and References

[a]*State Key Laboratory of Organic-Inorganic Composites, College of Materials Science and Engineering, Beijing University of Chemical Technology, Beijing 100029, P. R. China,* [b]*Changzhou Institute of Advanced Materials, Beijing University of Chemical Technology, Jiangsu 213164, P. R. China,* [c]*Aerospace Research Institute of Materials and Processing Technology, Beijing 100076, China. Fax: +86-010-64412084; E-mail: caiqing@mail.buct.edu.cn*

[1] H. B. Lu, F. Liang, J. H. Gou, J. S. Leng and S. Y. Du, *Smart Mater. Struct.*, 2014, **23**, 085034.

[2] H. B. Lu, Y. T. Yao, W. M. Huang and D Hui, *Compos. Part B*, 2014, **67**, 290.

[3] S. Lu, S. Li, J. Yu, Z. Yuan and B. Qi, *RSC Adv.*, 2013, **3**, 8915.

[4] Z. Wang, Z. Wang, H. Yu, L. Zhao and J. Qu, *RSC Adv.*, 2012, **2**, 2759.

[5] J. Liu, J. Tang, X. Wang and D. Wu, *RSC Adv.*, 2012, **2**, 5789.

[6] A. P. Mouritz, *Compos. Sci. Tech.*, 2012, **72**, 1568.

[7] S. G. Prolongo, M. R. Gude and A. Ure, *Compos. Part A*, 2012, **43**, 2169.

[8] W. Jiao, M. Shioy, R. Wang, F. Yang, L. Hao, Y. Niu, W. Liu, L. Zheng, F. Yuan, L. Wan and X. He, *Compos. Sci. Tech.*, 2014, **99**, 124.

[9] L. K. Grunenfelder and S. R. Nutt, *Compos. Sci. Tech.*, 2010, **70**, 2304.

[10] A. H. James, K. K. Sunil and R. J. Frank, *Compos. Sci. Tech.*, 2005, **65**, 1299.

[11] M. Bashar, U. Sundararaj and P. Mertiny, *Compos. Part A*, 2012, **43**, 945.

[12] G. Zhang, P. C. Lee, S. Jenkins, J. Dooley and E. Baer, *Polymer*, 2014, **55**, 4521.

[13] A. Khosravi, J. A. King, H. L. Jamieson and M. L. Lind, *Langmuir*, 2014, **30**, 13994.

[14] Y. Tokudome, T. Hara, R. Abe and M. Takahashi, *ACS Appl. Mater. Interfaces*, 2014, **6**, 19355.

[15] M. Yourdkhani, T. Mousavand, N. Chapleau and P. Hubert, *Compos. Sci. Tech.*, 2013, **82**, 47.

[16] H. Kang, K. Zuo, Z. Wang, L. Zhang, L. Liu and B. Guo, *Compos. Sci. Tech.*, 2014, **92**, 1.

[17] R. Ollier, E. Rodriguez and V. Alvarez, *Compos. Part A*, 2013, **48**, 137.

[18] A. C. Chinellato, S. E. Vidotti, G. H. Hu and L. A. Pessan, *Compos. Sci. Tech.*, 2010, **70**, 458.

[19] J. Xiong, Z. Zheng, H. Jiang, S. Ye and X. Wang, *Compos. Part A*, 2007, **38**, 132.

[20] F. Chivrac, E. Pollet, M. Schmutz and L. Avérous, *Biomacromolecules*, 2008, **9**, 896.

[21] G. B. B. Varadwaj, S. Ranab and K. M. Parida, *RSC Adv.*, 2013, **3**, 7570.

[22] M. M. Hasani-Sadrabadi, S. R. Ghaffarian and P. Renaud, *RSC Adv.*, 2013, **3**, 19357.

[23] J. K. Kim, C. Hu, R. S. C. Woo and M. L. Sham, *Compos. Sci. Tech.*, 2005, **65**, 805.

[24] G. Sui, W. H. Zhong, M. C. Liu and P. H. Wu, *Mater. Sci. Eng. A*, 2009, **512**, 139.

[25] L. B. Manfredi, H. D. Santis and A. Vázquez, *Compos. Part A*, 2008, **39**, 1726.

[26] X. L. Jia, G. Li, B. Liu, Y. Luo, G. Yang and X. P. Yang, *Compos. Part A*, 2013, **48**, 101.

[27] X. L. Jia, J. M. Zhu, W. B. Li and X. P. Yang, *Compos. Sci. Tech.*, 2015, **110**, 35.

[28] W. M. Chen, Y. H. Yu, P. Li, C. Z. Wang, T. Y. Zhou and X. P. Yang, *Compos. Sci. Tech.*,

2007, **67**, 2261.

[29] T. Glaskova and A. Aniskevich, *Compos. Sci. Tech.*, 2009, **69**, 2711.

[30] T. Ogasawar, Y. Ishida, T. Ishikawa, T. Aoki and T. Ogura, *Compos. Part A*, 2006, **37**, 2236.

[31] M. A. Rafiee, J. Rafiee, Z. Wang, H. Song, Z. Z. Yu and N. Koratkar, *ACS Nano*, 2009, **3**, 3884.

[32] X. Zhou, E. Shin, K. W. Wang and C. E. Bakis, *Compos. Sci. Tech.*, 2004, **64**, 2425.

[33] J. L. Suter, P. V. Coveney, H. C. Greenwell and M. A. Thyveetil, *J. Phys. Chem. C*, 2007, **111**, 8248.

[34] O. L. Manevitch and G. C. Rutledge, *J. Phys. Chem. B*, 2004, **108**, 1428.

[35] N. Sakairi, M. Kobayashi and Y. Adachi, *J. Colloid Interface Sci.*, 2005, **283**, 245.

[36] D. Sun, H. Cui and W. Sun, *Appl. Clay Sci.*, 2009, **43**, 485.

[37] L. Sophie, F. Delphine, P. Marc, R. Alain, R. Caroline and V. E. Luce, *Chem. Rev.*, 2008, **108**, 2064.

[38] M. Lipinska and J. M. Hutchinson, *Compos. Sci. Tech.*, 2012, **72**, 640.

[39] J. P. Yan, G. Yang, G. Xu and S. Y. Fu, *Compos. Sci. Tech.*, 2007, **67**, 2934.

[40] L. Madaleno, J. Schjodt-Thomsen and J. C. Pinto, *Compos. Sci. Tech.*, 2010, **70**, 804.

[41] S. M. Yuen, C. C. M. Ma, Y. Y. Lin and H. C. Kuan, *Compos. Sci. Tech.*, 2007, **67**, 2564.

[42] X. Xia, J. Yih, N. A. D'Souza and Z. Hu, *Polymer*, 2003, **44**, 3389.

[43] B. Guo, D. Jia and C. Cai, *Euro. Polymer J.*, 2004, **40**, 1743.

[44] H. Li, Y. Yu and Y. Yang, *Euro. Polymer J.*, 2005, **41**, 2016.

[45] T. Ogasawara, Y. Ishida, T. Ishikawa and R. Yokota, *Compos. Part A*, 2004, **35**, 67.

[46] X. Wang, J. Jin and M. Song, *Carbon*, 2013, **65**, 324.

TOC

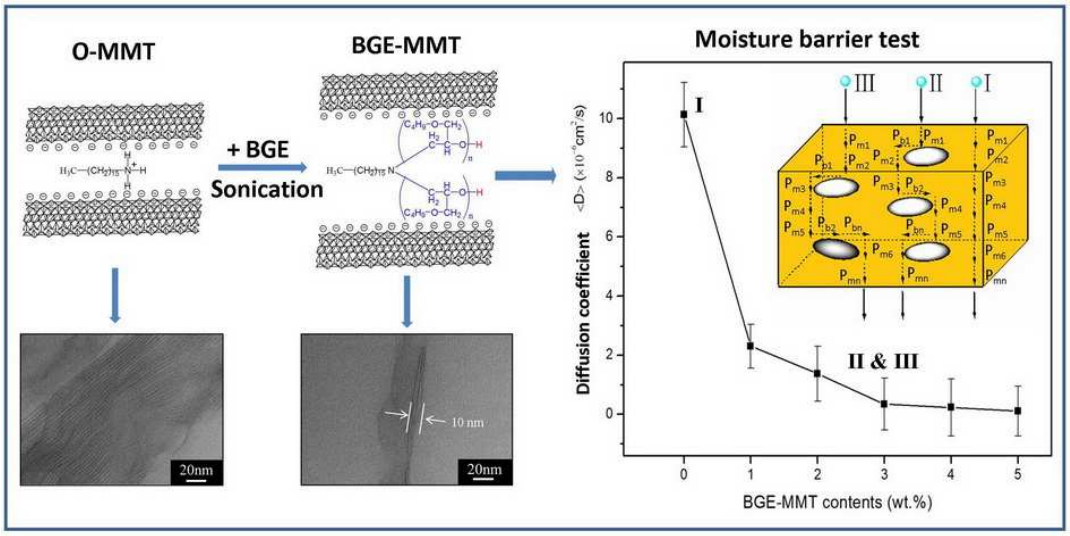

A one-step reaction approach was exploited to prepare an activated liquid nano-reinforcement (BGE-MMTs) for enhancing moisture-barrier characteristics of epoxy composites.